690

Study of Hadronic Production and Spectroscopy
of Strange, Charm and Bottom Particles at the Tevatron

M. Church, S. Holmes, B. Knapp Spokesman

Nevis Laboratories, Columbia University, Irvington, NY 10533

D. Jensen, M. Kreisler, M. Marcin,
M. Rabin, K. Raychaudhuri

Department of Physics, University of Massachusetts,
Amherst, MA 01003

C. Avilez, B. Fuentes, M. Oreno

Instituto de Fisica, University of Mexico,
Mexico 20, D.F., Mexico

January 1981

DIRECTOR'S OFFICE
FEB 3 1981

Table of Contents

	Page
I. Introduction	1
II. Physics	
A. General Physics Goals	3
B. Diffractive Dissociation	6
C. Hard Collisions	10
III. Detector	11
A. Magnetic Spectrometer	12
B. Photon and Hadron Calorimeter	15
C. Charged Hadron Identification	17
D. Lepton Identification	18
E. Vertex Resolution	19
F. Detector Electronics	20
G. Online Reconstruction	20
IV. Measurement Program	
A. Phased Development of Full Detector	22
B. Study of Target Fragmentation into Massive States	
C. Target Dissociation Rates	26
D. Physics Measurements with the Full Detector	31
Requests, Costs, Schedule	33
References	35
Tables	37
Figures	43

I. Introduction

We propose to study the spectroscopy of strange, charm and bottom particles and their production in collisions of high energy hadrons with stationary targets. To accomplish this study, we must build a special forward spectrometer, capable of unusually accurate and complete reconstruction of complex multiparticle reactions at startlingly high rates. We anticipate reconstruction of at least 10^5 events per second at interaction rates in excess of 10^6 per second. This detector will be uniquely capable of mining a wealth of elementary particle physics which will otherwise remain relatively untouched. As an example of the power of this technique, we expect data rates of at least 10^4 fully reconstructed charm pairs per hour, fully isolated and identified.

This proposal is a direct descendant of Fermilab Proposal 627, which we recommend reading for its discussion of measurement problems and solutions. We have improved the design of the magnetic spectrometer to measure an even larger dynamic range of reaction products. Furthermore, this spectrometer can be built up more gradually, with a steadily productive and improving measurement program. We now propose a series of measurements in a charged hadron beam with energy variable up to full Tevatron primary beam energy. Although we hope eventually to propose later experiments using this detector to study interactions of high energy photons, we feel that

charged hadrons offer much higher signal rates with a much simpler beam. The detector will have such general measurement capability that experiments should eventually span a range of beams and targets.

We can efficiently use the high interaction rates available in hadron beams to measure reactions as rare and complex as charm production with high signal rates and little background. The domination of "new particle" physics by e^+e^- annihilation experiments, despite their vanishingly low rates, has long been explained by the existence of large "backgrounds" in external beam reactions, particularly in hadron-hadron collisions. These "backgrounds" do not reflect any intrinsically undesirable properties of hadronic reactions but rather quite correctable limitations of individual experiments. Two distinctly different problems are frequently labelled "background". The first is simply the saturation of measurement rate at unpleasantly low signal levels as a result of limitations on the amount of offline computation, the speed and selectivity of online event selection, or even the resolving time of the detector. A second problem arises when otherwise readily isolated signals are inadequately measured. We have solutions to both of these problems, and we hope to demonstrate that detailed measurements of both new and old physics are practical on a scale well beyond present experience.

II. Physics

A. General Physics Goals

We wish to study the production and spectroscopy of strange, charm and bottom particles. Our initial goals include:

1) systematic study of exclusive reactions, particularly diffractive dissociation,
2) a simple catalogue of the remaining stable charm particles, with details of production and decay,
3) determination of the scale of bottom production in hadron collisions.

We ultimately expect to accurately measure lifetimes, branching ratios and production cross sections, as well as observe excited states and additional production details for all S, C and B production by hadrons.

Since we will begin this experimental program a decade after the discovery of the ψ,[1] and two decades after the discovery of the last stable strange particle,[2] one might reasonably wonder just how much of what we could measure would still be of interest to the physics community by the time we could measure it. Despite occasional rumors that all of elementary particle physics is now well understood, very little detail has actually been measured, and we can predict quite safely that relatively little detail will appear until an experiment such as we propose has actually been conducted.

With the extension of the original three quarks of SU_3 to at least five, one expects a large spectrum of hadron

states which is largely unexplored.[3] Of the large number of stable charm particles predicted, only D mesons and the Λ_c have been firmly established, and they were discovered in e^+e^- annihilation experiments,[4] where the rates are simply too low for significant chance of additional such discoveries. Detection of these particles in photoproduction and hadron reactions has been difficult, with a few mass bumps of modest statistical significance or a few probable observations of the finite lifetime of short-lived particles.[5] No real measurement of production cross sections or establishment of new states has been possible in either hadron or photoproduction experiments so far. We expect the rarity and complexity of signals to continue to limit the results of conventional experiments in external beams.

Surprisingly enough, even detailed measurement of $S\bar{S}$ production does not now exist, for many of the same reasons that significant observations of charm production in hadron interactions have proven elusive: namely, that specific signals are too complex and rare for traditional measurement techniques. The single most extensive study of exclusive strange particle production is a bubble chamber study of 10-25 GeV neutron interactions in hydrogen,[6] with observation of a few events in each of a long but very restricted list of exclusive reactions with a V^o and no missing neutrals.

Because we will be able both to measure the information necessary to reconstruct the exclusive, or partially inclusive, final states, and also to isolate and record these events at

high rates, we will for the first time ever be able to record a long list of such reactions with very high statistics. Such measurements are desirable for a variety of reasons: in the first place any measurement of charm and bottom production calls for strong constraints to exclude backgrounds and high rates to obtain signals, and secondly we think it unlikely that details of strong interaction dynamics can be discovered in purely inclusive measurements. Isolation of resonances in strange, charm and bottom systems may prove particularly informative. If the excitation spectrum of the $C\bar{C}$ and $B\bar{B}$ systems is any indication of what we may encounter in heavy quark systems,[7] we may very well encounter a rich readily interpretable spectrum of states which would lead to a simple understanding of at least the low energy interactions of their constituents.

To get some idea of what measurements might be practical, let us first see what information might be present in collisions of energetic hadrons with fixed targets at the Tevatron. Present expectations of C and B production cross sections still await firm measurement, but are expected to be of order 10^{-3} and 10^{-5} of the total cross section.[8] With a target thin enough for multiparticle measurements, 5% interaction length, we expect to cope with 1 MHz interaction rate and 20 MHz charged beam particles. With a thousand seconds of beam expected per hour of Tevatron operation, <u>hourly</u> interaction rates become a billion total interactions,

including a million charm pairs and ten thousand bottom pairs.

Of course, the available information varies dramatically from event to event. Even though relatively unconstrained measurements with high backgrounds may prove useful with high statistics, the most useful events will be not only fully reconstructed but also in special kinematic regions. As we describe below, we expect our ability to reconstruct the majority of individual charm particle decays to combine with an estimated ten to twenty percent of the total charm production appearing in readily isolated reactions to yield well over 10^4 fully reconstructed and fully isolated charm pairs per hour. Fortunately, these will be spread over an enormous number of different topologies and reactions.

B. Diffractive Dissociation

We wish to study fully reconstructed diffractive single dissociation reactions for a variety of reasons: they offer an opportunity to study an incredibly wide range of hadronic states in the simplest possible reactions, with the greatest isolation from other phenomena and with strong measurement constraints. Although there is no universally accepted definition of such reactions, diffractive quasi-two-body reactions account for at least half of the hadronic total cross sections.[9] Such reactions include elastic scattering, single dissociation and double dissociation. Diffraction phenomena are present in most of the total cross section, in the small P_T behavior of inclusive single particle production,

for example. Such effects are to be expected in the production of finite sized objects in collisions of similarly large objects.

Single dissociation reactions can be written as

$$h_1 + h_2 \rightarrow h_1 + X$$

where a collision between two hadrons h_1 and h_2 results in little four-momentum transfer to hadron h_1 but hadron h_2 breaks up into system X with mass M_X. Missing mass measurements that rely only on measurement of the outgoing hadron h_1 have been performed for various hadrons at several energies.[9-15] Although the various measurements appear consistent with each other, their interpretations differ greatly, with varying parameterizations and estimates of diffractive dissociation. Experiments with adequate resolution see structure in the region of M_X^2 between 2 and 4 GeV^2, with little variation of $M_X^2 \frac{d\sigma}{dM_X^2}$ with M_X^2 between 4 and 10 GeV^2. The broadest study was reported for pp and πp collisions in the Fermilab bubble chamber,[10] with reported missing mass distributions shown in Fig. 1. An internal target experiment at Fermilab reports a simple parameterization of the missing mass cross section for pp collisions over a wide range of missing mass and center of mass energy:[14]

$$\frac{d\sigma}{dM_X^2} = (3.8 \pm 0.3)/M_X^4 + (15.7 \pm 1.1)/s \quad mb/GeV^2 .$$

All of these experiments identify the low mass enhancement as diffractive single dissociation, but they are unable even

in principle to determine what fraction of the missing mass spectrum is single dissociation. The ISR experiment reporting a total cross section for single dissociation did not rely solely on missing mass, but included all $M_X^2 < 0.1$ s in which the undissociated proton appeared alone in its hemisphere.[9]

Elastic scattering and single dissociation appear to approach constant cross sections at high energies, presumably the result of similar energy-independence of more inelastic cross sections rather than an intrinsic property of diffraction. Proton dissociation into $p\pi^+\pi^-$ [16] and ΛK^+ [17,18] have now been measured over a wide range of energies. These reactions are clearly diffractive single dissociation and fall with increasing energy to a constant cross section at ISR energies, with an energy dependence quite consistent with missing mass measurements. On the other hand, the entire inelastic cross section cannot be usefully considered to be single dissociation. We might expect to identify proton diffraction into bottom pairs with $M_X^2 = 125$ at $s = 500$, but we would not consider all reactions with $M_X^2 \leqslant 0.25$ s to be single dissociation.

We suspect that approximately 20% of the total production of S, C and B particles occur as single dissociation into low multiplicity states, but such reactions have never been systematically measured and could be less frequent than we estimate. The overall rates and background rejection are nevertheless sufficiently high that we can study S, C and B physics at production levels well below our estimates. We

assume, for example, that strange particle production in single dissociation is approximately 800 μb at high energies, but the only two measured reactions, $pp \rightarrow p\Lambda K^+$ and $pp \rightarrow ppK^+K^-$, account for only 8-10 μb and 2 μb, respectively, at the ISR.[18] On the other hand, the lower energy bubble chamber measurement of exclusive reactions reports a long list of reactions with larger cross sections, and reports strong evidence for diffractive dissociation in most of these reactions.[6] When one considers the large number of S = 1 baryon and meson states that should be produced with comparable frequency, the possibility that proton dissociation into ΛK^+ is only 1% of dissociation into $S\bar{S}$ seems quite plausible.

As for charm production, even less has been clearly measured. Reported observation of pion dissociation into $D\bar{D}$ in 200 GeV πp interactions at Fermilab,[19] with an estimated cross section of 6-10 μb, and reported observation at the ISR of large forward production cross sections for charm particles,[20] consistent with diffractive dissociation, all support our assumption. On the other hand, all of these experiments report small single particle mass bumps with large backgrounds.

One might conclude that diffraction is fundamentally a low mass phenomenon, and that particles as massive as charm or bottom particles are best sought elsewhere, perhaps the central region or at high P_T. In fact, the total cross section is dominated by low mass phenomena, and diffractive

dissociation allows one to isolate relatively rare fundamentally massive phenomena. Because the mass spectrum for dissociation falls so rapidly, and because S, C and B production turn on at progressively higher masses, we expect them to be fair fractions of possible candidates. We thus expect absolutely negligible background to isolation of charm production, which should be at least a few percent of dissociation into sufficiently massive states, with multiplicities comparable to strange particle production. The two charm particle mass constraints should provide rejection factors of 10^{-3} to 10^{-5} for massive strange particle production. The relatively low multiplicities minimize the combinatorial backgrounds.

C. Hard Collisions

Complete event reconstruction is not restricted to low multiplicity quasi-two-body reactions. We have excellent acceptance out to the kinematic limits for high mass or high transverse momentum. We can reconstruct jets of modest multiplicity in reactions with moderate multiplicity ($\sim$ 20 particles). Such reactions are easily selected with a calorimeter trigger. Note that we anticipate reconstruction of up to 10^8 events per hour chosen from 10^9 interactions.

III. Detector

The physics measurements which we propose are possible only with a very powerful detector. The full detector is shown in Fig. 2 and described in some detail in Tables 1, 2 and 3. In particular, the detector which we propose is capable of:

1) efficient detailed measurement of very complex reactions,

2) performing the traditional fast trigger function - selection of desired events - with very high efficiency, even when the desired signature is very complicated,

3) operation in the presence of tens of millions of detectable particles per second,

4) supplying, in useful form, considerably more information than is normally available for offline analysis.

Both the amount of information measured in individual reactions and the rate at which measurements can be performed are unusually high. For most of the center of mass phase space, particularly the forward hemisphere, we accurately and efficiently identify and measure all charged particles, photons and neutral hadrons. Decays of strange particles, including $K_S \rightarrow \pi^+\pi^-$, $\Lambda \rightarrow p\pi^-$, $\Xi^- \rightarrow \Lambda\pi^-$ and $\Omega^- \rightarrow \Lambda K^-$ (as well as the antihyperons), are efficiently reconstructed over very nearly all phase space. Directions of neutrals are determined with precision comparable to charged particle measurements, but energies, particularly for neutral hadrons

(K_L, n and $\bar{n}$), are less precisely determined. Identification of charged hadrons (πKp) represents a significant advance over any previous experiment.

A. Magnetic Spectrometer

We have designed a magnetic spectrometer capable of rapid efficient measurement of charged particles in complex multi-particle reactions over a very large dynamic range. The spectrometer, shown in Fig. 2 and described in Table 1, uses two analyzing magnets and a series of 9 drift chamber modules. Particle momenta are measured with an accuracy of a fraction of a percent over a momentum range of 200 MeV to 100 GeV. Particles with decreasing momentum and increasing lab angle require progressively less of the spectrometer for accurate measurement. For 400 GeV beam particles, for example, the only center of mass kinematic region not covered is the most backward 1% of the full solid angle, and that only for extremely relativistic particles, with $\beta\gamma$ at least 10 in the center of mass. Of course, such particles are not uncommon, particularly in dissociation reactions where the target system acquires little mass, but we accept strange, charm and bottom production everywhere, including the target fragmentation region.

We have located a CEA spectrometer magnet, the "Jolly Green Giant", which has lain idle in a storage yard at Brookhaven for the past decade. This magnet is ideal for a first magnet "outer detector", covering a large solid angle and permitting measurements with chambers at depths within the magnetic field

which increase with particle momentum. This magnet has an aperture 8-ft wide, 4-ft high, and 7-ft deep. Its pole faces, however, are only 5-ft wide and 4-ft deep, resulting in a smoothly varying field with a relatively small volume at nearly peak magnetic field. Only because particles entering the magnet see an increasingly strong field can our simple configuration easily measure such a large momentum range. We would operate the magnet at 8 kG peak field, or a total field integral of 400 MeV, with about half its original megawatt power consumption.

The second magnet would be a new magnet, with an aperture 4-ft high, 5-ft wide and about 6-ft deep, with a field integral of 600 MeV. Although this magnet could be a conventional pictureframe dipole, we would like to investigate alternate designs to see if a more convenient coil configuration is practical and whether the return yoke could be segmented to permit calorimetry and muon identification. We suspect that a transformer-style coil configuration is feasible, with an increase in copper for fixed power consumption offset by ease of construction, and with the advantage that the coils would not interfere with the upstream photon detector or the downstream Cerenkov counter optics, permitting a more compact geometry for fixed field volume.

The 9 drift chambers each consist of 3 planes measuring the horizontal bending of the charged particles, with 1 vertical plane and 2 planes rotated away from vertical by $\pm 15^{\circ}$. These

drift chambers are highly segmented to permit efficient high speed measurement of crowded reactions at high interaction rates. The anode wire spacings range from 2 mm in the first 2 chambers to 6 mm in the last chamber. We use a purely digital TDC which measures the time of the first signal on each wire with time bins of 2.5 ns width, with ability to read out measurements at 20 MHz per plane. The chamber memory times range from 60 to 100 ns, so that with a diverging beam of 1 to 2 inches in diameter, we can cope with 20 MHz charged beam particles and 1 MHz interaction rate.

We have studied track reconstruction for this detector in considerable detail. We have developed excellent algorithms for conventional Fortran track reconstruction and for hardware reconstruction. We have already tested a fast Fortran reconstruction program and conducted Monte Carlo studies of resolution and efficiency. Speed and efficiency benefit considerably from sufficiently fine wire spacing that pattern recognition does not depend on ambiguous and relatively inefficient drift time measurements.

Track reconstruction is similar to that of Experiment 87A. Tracks are first located in single views, with poor resolution but with adequate speed and efficiency. Tracks appearing in two different views with the same momentum define a single track in all planes with sufficient resolution to initiate an iterative least-square fit in which left-right ambiguities associated with drift times are quickly resolved. As before,

we first find stiff highly constrained tracks passing through a majority of the chambers, and then pick up less constrained tracks. We locate all tracks above 5 GeV in the last 6 chambers, all above 1 GeV in the first 6 chambers, all remaining tracks in three sets of four contiguous chambers, and finally any remaining soft, wide tracks in the first three chambers. This yields very nearly all reconstructable charged particles, including decays of stable particles. Decays of $K_S \rightarrow \pi^+\pi^-$, $\Lambda \rightarrow p\pi^-$, $\Xi^- \rightarrow \Lambda\pi^-$ and $\Omega^- \rightarrow \Lambda K^-$ are highly constrained and efficiently reconstructed, as are decays of the corresponding antihyperons. The decays of $\Sigma^\pm$ are efficiently reconstructed as strongly kinked tracks, but require observation of the neutral decay particle.

B. Photon and Hadron Calorimeter

Immediately downstream of the magnetic spectrometer we measure the conversion points and energies of photons and hadrons with a large highly segmented calorimeter, described in Fig. 2, in which showers developing in lead and iron are sampled with wire proportional counters. The calorimeter would have an active aperture 8-ft square, with a 4-sq in. hole for uninteracted beam particles. This detector must tolerate interaction rates above 10^6 per second and resolve closely spaced particles in high multiplicity reactions.

Good resolving power is particularly vital for the multiparticle measurements we wish to make. This requires both highly segmented sampling and limited shower dimensions.

We presently favor a design similar to that developed for the MAC detector at PEP,[21] with layers of Pb alternating with extruded aluminum ribbed sheets that provide small rectangular cross section tubes, each of which would then contain a single proportional counter anode wire. To reduce the memory time of the counter and to maximize its density, thereby minimizing shower spread, we would keep the sampling volume as small as practical, with about 6 mm of sampling structure separating the lead sheets. Such a structure would be slightly faster and twice as dense as the counter described in Proposal 627. The sampling would be segmented first into separate 4-ft square quadrants, which are segmented into 1 cm vertical and horizontal strips. The photon calorimeter would be segmented longitudinally into three units of eight radiation lengths each, with sampling every half radiation length. The total number of analog charge measurements is 3,000, or 500 per view for each longitudinal sample. With this calorimeter, we should at least equal the performance of the detector tested for Proposal 627, or $24\%/\sqrt{E}$ r.m.s. energy resolution and 2 mm spatial resolution, with resolution of showers separated by 1 in. or more, over a moderate range of relative energies.

The photon calorimeter has roughly 50% detection efficiency for neutral hadrons, which typically deposit little energy upon interaction, but instead initiate a relatively broad and penetrating shower. We would follow the photon

calorimeter with two more sections identical to the photon detector, except that each contains 16 layers of 6 mm iron. Most neutral hadrons will thus be detected with transverse coordinates localized to within a few mm. To measure the hadron energy, the hadron interaction detector is followed by a conventional iron plate calorimeter with shower sampling provided by proportional counter planes with cathode readout in a 32 x 32 rectangular grid. The total number of analog measurements in the photon and hadron calorimeter is 6,000.

C. Charged Hadron Identification

Distinguishing among the stable charged hadrons in multiparticle states at Tevatron energies is probably the most difficult technical challenge we presently face, but we are not alone in this respect. Practical procedures for identifying hadrons above 50 GeV should be found within the next few years. For the moment, however, we rely on techniques we understand today and continue to use segmented threshold Cerenkov counters. This has the primary advantage of restricting final state particles to momenta less than 50 GeV for π, K identification and less than 100 GeV for proton identification.

The 3 Cerenkov counters, described in Table 3, have pion threshold momenta of 3, 6 and 12 GeV. They are atmospheric pressure counters segmented as much as practical with conventional 2-in. phototubes. We use rectangular arrays of

spherical mirrors to reflect Cerenkov light onto rectangular baffles which direct photons with at most one grazing-incidence reflection onto a photocathode. The two smaller counters require aluminized mylar plane mirrors to deflect the light to spherical mirrors outside the active aperture of the spectrometer. For long life and quick recovery, the phototubes will be operated at relatively low gain, with limiting amplifiers in the phototube bases.

The measurement of the Cerenkov light is segmented twice, first by the individual photon's apparent coordinate at the midplane of the counter and then by its coordinates at the spherical mirror array. This scheme permits a considerable reduction in confusion in multiparticle reactions at a cost similar to more conventional Cerenkov counter segmentation with fewer but larger phototubes.

D. Lepton Identification

Electrons will be identified by the photon calorimeters. Low energy electrons, below 3 GeV, can be identified in the first Cerenkov counter. Dalitz pairs and Bethe-Heitler production in the target can be very efficiently identified, with the very wide dynamic range of the magnetic spectrometer providing efficient detection of low energy electrons in very asymmetric pairs.

Muons will be identified by lack of interaction in several interaction lengths of highly segmented calorimeter.

For an additional positive signature of non-interaction, we follow the calorimeter with concrete and two planes of multiwire proportional chamber. Decays in flight of pions and kaons are largely suppressed by trajectory measurement.

E. Vertex Resolution

With the chamber system described above, we will be able to detect and measure lifetimes on the order of 10^{-13} seconds. Not only does that ability permit accurate determinations of charm and bottom decay parameters but it presents an additional constraint possibly extending the kinematic conditions under which such particles are measurable.

In the portion of the program investigating dissociation physics with a long hydrogen target, Monte Carlo calculations indicate that our resolution in $c\tau$ should be $\leqslant$ 0.1 mm for $\Lambda_c \rightarrow pK^-\pi^+$, $D^o \rightarrow K\pi$ and $D^{\pm} \rightarrow K\pi\pi$. We see two straightforward ways to make significant improvements in that resolution for future parts of this program: (a) When studying dissociation from short nuclear targets, we will add a high pressure drift chamber directly downstream of the target, yielding at least a factor of 5 improvement in vertex resolution. (b) Eventually we hope to utilize a fully instrumented target such as the silicon targets currently under development.

F. Detector Electronics

Because we wish to reconstruct 10^5 interactions per second with low deadtime, we require that all measured information be transferred within 1 μs, freeing the detector for another measurement. All fast electronics except simple discriminators would be of Nevis design. An inexpensive drift chamber TDC capable of supplying at least 20 measurements per plane within 1 μs has been tested and is being supplied in quantity to Fermilab Experiment 605. Relatively minor design modification of an inexpensive 12-bit ADC, more than 6,000 of which have been supplied to other experiments, will permit analog measurements to be buffered within 1 μs for subsequent digitization with 10 μs. Time of flight measurements will be made with similar devices in which a linear gate is replaced by a gated time to voltage converter. The drift chambers will have 8-channel preamplifiers mounted on the chambers and cabled to 32-channel amplifier discriminators nearby, which in turn drive long delay cables to the 6-bit TDC system.

G. Online Reconstruction

We have developed at Nevis a simple approach to fast digital computation which will allow us to reconstruct online at least 10^5 multiparticle reactions per second, accurately, inexpensively, and in as much detail as we find necessary. This approach is described in some detail in an addendum to Proposal 627.

The most important features of the processor we summarize here. It is a synchronous pipeline structure in which an enormous number of very simple computations are performed simultaneously. A clocked system with a well defined sequence of states, it can be simulated exactly with a simple Fortran program. The actual elapsed time before an event is sufficiently reconstructed for a trigger decision may be several tens of microseconds, but a new event can enter the pipeline every 10 μs. The computation can be modified or expanded easily at any time. Operation and maintenance are simple and reliable.

IV. Measurement Program

A. Phased Development of Full Detector

The proposed detector is sufficiently complex that one might worry about the time scale, particularly the amount of beam time, required for the construction of the many large components and their successful integration into a working detector. We propose a multistage program which will allow both detector and beamline to develop continuously from relatively modest beginnings, with a steadily productive physics program. We would begin with a study of target proton dissociation into massive all charged particle states that would require little more than the upstream portion of the magnetic spectrometer.

We would start with the system shown in Fig. 3, consisting of the upstream magnet, six drift chambers, a single threshold Cerenkov counter, some scintillation counters for trigger and time of flight measurement, and of course the nucleus of the eventual data acquisition system, including online track reconstruction. We have proposed using this simple spectrometer to study strange and charm particle production at the Brookhaven AGS (Proposal 766). This would permit us to bring to Fermilab a working tested spectrometer at the earliest availability of a suitable experimental area, presently estimated as late 1984. Once installed in a high energy charged hadron beam at Fermilab, this detector would permit an immediately productive and steadily improving experiment, with online reconstruction providing access to incredibly

high signal rates at every stage.

To overcome the long lead times associated with construction and installation of most of the large components of the full spectrometer, we would construct the full spectrometer concurrently with the first stage measurements. Installation of downstream elements would benefit from the existence of the upstream detector, which could calibrate and generally check out any new elements. New downstream elements could not interfere with upstream measurements, but would instead add enormously to overall measurement capabilities once they have been integrated into the detector.

B. Study of Target Fragmentation into Massive States

For the special kinematics of target fragmentation into massive states, little more than the upstream portion of the spectrometer is necessary for the isolation and measurement of exclusive all charged particle topologies. The upstream spectrometer measures charged particles with lab momenta as low as 200 MeV for lab angles out to 45°, and out to 300 mrad for particle momenta above 1 GeV, with momentum resolution $\delta p/p \leqslant 0.01$ at 10 GeV. The single threshold Cerenkov counter C_0 identifies pions between 3 and 10 GeV. Scintillation counters at the fourth and sixth drift chambers provide time of flight identification for particles with velocities up to 0.75 and 0.9, respectively.

To isolate the exclusive reactions, we must also know the incoming and outgoing beam particle directions and momenta with sufficient precision to permit measurement of overall transverse momentum conservation to within 30 MeV and longitudinal momentum conservation to within a few percent. Measurement of the outgoing particle requires a second small magnet, with roughly 6-in. square aperture and a few hundred MeV transverse momentum kick, 50 ft downstream of the spectrometer, and followed by 3 small drift chambers with 2-mm wire spacing.

The result is a strong four-constraint fit for fully reconstructed target dissociation reactions. The two transverse momentum constraints suppress reactions with undetected particles. Longitudinal momentum conservation further suppresses reactions with undetected forward particles. The fourth constraint, best expressed as conservation of $E-P_L$, suppresses reactions with missing or improperly identified target fragments.

This fourth constraint insures accurate measurement of the mass M_X of the target fragmentation system without requiring particle identification and also insures efficient reliable particle identification. For the relatively low momentum target fragments, the value of $E-P_L = (m^2+P_T{}^2)/(\sqrt{m^2+P^2} + P_L)$ depends noticeably on particle mass m. The sum of this quantity over all target fragments must add up to the target proton mass to within experimental resolution of a few MeV.

We wish to measure reactions of the type

$$b + p \rightarrow b + X$$

where the high energy beam particle b loses a small fraction of its energy to the target system and acquires a momentum P_T transverse to the original beam particle direction. If the outgoing beam particle is sufficiently energetic that its $E-P_L$ is negligible compared to m_p, we find that

$$M_X^2 = m_p(2P_L + m_p) - P_T^2$$

where the directly measured quantities are the momentum components of the target system, P_T and P_L, both measured with high precision. Measurement of the outgoing beam particle also provides an accurate measurement of P_T and a coarse measurement of P_L. Note that particle identification is not required. The expression can be inverted to yield P_L in terms of M_X and P_T, demonstrating that the appearance in the lab of the target system is quite independent of beam momentum, for high beam momentum:

$$P_L = (M_X^2 + P_T^2 - m_p^2)/2m_p \quad .$$

One might also note in passing that for very high mass systems containing bottom pairs, the target fragmentation is well matched to the full spectrometer so that detection of neutrals will be possible, and that complete hadron identification will be straightforward without an imaging Cerenkov counter, even for TeV beam particles.

Although not comparable to the acceptance of the full spectrometer for forward production, the acceptance of the upstream magnet system for charged particles from target fragmentation is quite respectable for strange and charm production. In Table 4, we list Monte Carlo computation of detection efficiency for specific reactions, where we have assumed $d\sigma/dP_T^2 \propto e^{-7P_T^2}$ and all particle decays have isotropic Lorentz invariant phase space distributions.

C. Target Dissociation Rates

The selection of desired target dissociation events is almost within reach of conventional fast trigger logic. We should be able to obtain an efficient trigger with no more than 10% deadtime, selecting fewer than 10^4 events per second at interaction rates of 10^6 per second and 2×10^7 beam particles per second. With online track reconstruction hardware designed for much higher event rates, we anticipate little difficulty isolating the one hundred most attractive events each second. We first isolate fully reconstructed reactions by requiring overall transverse momentum conservation. We should then be able to select events solely on the basis of the mass of the target system, strictly a function of its observed laboratory momentum. Although available, online particle identification and vertex reconstruction should not be necessary. From the missing mass measurements, we expect about 1% of the interactions to have M_X between 4 and 6 GeV, for example, but fewer than 1% of these should result in fully reconstructed all-charged particle states.

To obtain an event trigger, we first require a three-fold coincidence between a small beam counter and the two time of flight hodoscopes, located outside the beam envelope immediately behind drift chambers 4 and 6. This provides a gate signal for fast coincidence register logic, with roughly 10^6 per second and less than 100 ns deadtime. We select target dissociation by then requiring at least one beam particle within the downstream spectrometer, which has acceptance only for $\Delta\theta \leqslant (1\ \mathrm{GeV}/P_{beam})$ and $\Delta P/P_{beam} \leqslant 0.2$. We would also veto any event with more than 10 GeV deposited in a small electromagnetic shower counter, 24 in. diameter with 6 in. beam hole, immediately upstream of the small beam magnet. To select candidates for reconstructable target dissociation, we also require the presence of charged particles in the drift chambers and the absence of detectable particles, including photons, in the vicinity of the target but outside the spectrometer acceptance.

If we assume that target dissociation into charm is 10^{-4} of all interactions, we expect 100 such events per second or 10^5 per hour. But with fewer than 10% of the decays of individual charm particles reconstructable, and with detection efficiency typically 20% for states without unobservable neutrals, we expect between 10 and 100 fully reconstructed charm pairs per hour.

Although this is fully three orders of magnitude lower than we would expect for measurement of beam particle

fragmentation with the full spectrometer, with its greater detection efficiency and efficient measurement of neutrals, these reactions are sufficiently constrained that we can measure them in detail with negligible background. We assume that target dissociation into strange particles is 400 μb. The backgrounds that these reactions present to charm production are completely negligible. Even though charm production is a factor of 100 smaller, it occurs at values of M_X higher than most of strange particle production and can be separated from possible background with at least a factor of 10^4 rejection arising from the two charm particle mass constraints. The lowest multiplicity strange particle reactions are not candidates for charm production. The higher multiplicities suffer the same inefficiencies that reduced charm detection.

The usually deadly combinatorial amplification of backgrounds is also largely absent, for a variety of reasons. First of all, every single hadron is identified unambiguously, eliminating the usual multiple choice guessing game based on measurements in which most particle identities are unknown, but one or two particles have been isolated as not-pions. Secondly, the single dissociation reactions have the lowest possible multiplicity, either with the production of relatively unaccompanied charm particles, with at most a few combinations per event, or with the production of charm particle resonances to provide additional very strong constraints. For example, the relatively low multiplicity

reactions $p \to pK^+K^-\pi^+\pi^-$ and $p \to \Lambda K^+\pi^+\pi^-$ are each candidates for $p \to \Lambda_c\bar{D}^o$ with only one combination each. Among the highest multiplicity candidates for $p \to \Lambda_c\bar{D}^o$ is $p \to (\Lambda\pi^+\pi^+\pi^-)$ $(K^+\pi^+\pi^-\pi^-)$ with nine combinations.

Because individual charm particles have more than one reconstructable decay mode, we expect specific production reactions to show up in several topologies. For example, in 200 hrs., if the target fragmentation reaction $p \to \Lambda_c\bar{D}^o$ is 40 nb (10^{-6} of all reactions, 10^{-3} of charm production), we expect a total number of reactions $p \to \Lambda_c\bar{D}^o \to pK^+K^-\pi^+\pi^-$ of (0.25) $(0.02)^2(10^{-6})(2 \times 10^{11})$ or 20 events. To estimate background from this topology, note that the entire topology accounts for less than 10^{-4} of all interactions, with a mass spectrum strongly peaked below 3 GeV, falling sufficiently rapidly above 3 GeV that we expect only about 1% to lie above charm threshold. For masses $M(pK^+K^-\pi^+\pi^-)$ above 4.2 GeV, the $M(pK^-\pi^+)$ and $M(K^+\pi^-)$ should be broad but peaked at low masses, particularly $M(K^+\pi^-)$, so that the region within 10 MeV of the $(M(\Lambda_c), M(\bar{D}^o))$ point in the two dimensional distribution should contain less than 10^{-5} of the total. Additional restrictions, such as exclusion of $\phi \to K^+K^-$, can help further. Assuming the same detection efficiency as for the charm production reaction, we predict less than 0.5 event background from this topology. Other topologies should have comparable signal-to-noise ratios, so that, if we include other detectable decay modes of Λ_c and $\bar{D}^o$, we expect a few hundred events with at

most a few background events. For $p \to \Sigma_c^{++} D^{*-} \to (\pi^+ \Lambda_c)(\pi^- \bar{D}^o)$, to take an extreme example, we expect comparable signal, but the cascade decays provide additional constraints that suppress backgrounds by roughly another factor of 10^{-5}.

Note that detection efficiency, constraints and overall rate generally conspire to permit measurement of target dissociation into some quite exotic states at the level of a few events per picobarn. In addition to simple associated production of strangeness or charm, we should see reactions like $X \to p\Omega\bar{\Omega}$ and possibly $X \to p\Omega_c\bar{\Omega}_c$. Until we can see neutrals, however, each additional charm pair will be accompanied by a decrease in detection efficiency at least as great as the decrease in cross section. Without neutrals, we can hope to observe multiply charmed particles with detectable cascade decays to singly charmed particles, but not production of two charm particle pairs. For target dissociation to bottom pairs, the low cross section and high multiplicity expected do not leave much room for optimism about detection of individual bottom particles without neutral detection, but with target dissociation into bottom pairs expected at the level of 10^3 per hour we may be able to detect an enhancement near $M_X = 11$ for dissociation into massive states with moderately isotropic decays into several strange particles.

D. Physics Measurements with the Full Detector

As the various pieces of the full detector are finished, they will be added to the spectrometer. We stress again that the addition of these pieces will add enormously to the physics measurement prowess of the experiment independent of which pieces arrive first. For example, the existence of the photon detector would significantly augment the capabilities of the spectrometer as soon as it is online. Thus, the physics program would not only be productive initially but would expand toward the capabilities of the full detector yielding ever more interesting physics during the transition. Instead of discussing the measurement program for different apparatus construction schedules, we summarize below the program we currently foresee for the full detector.

The goals of the measurement program are to study the production and spectroscopy of strange, charm, and bottom particles. Initially, we will be concentrating on diffractive exclusive reactions to accomplish these goals.

Assuming that the total charm cross section is 10^{-3} of the total cross section and given 20 MHz charged beam and a 1 MHz interaction rate, we estimate that we will fully reconstruct and isolate 10^4 charm pairs per hour. We stress that these rates are observed decays including all branching ratios. We note that these rates are significantly higher than previous experience. However, it is just that high rate coupled with our trigger selectivity which will allow us to meet our goals.

In the course of a 1000 hour run with the full detector, we would record some 10^7 charm pairs and perhaps as many as 10^5 bottom pairs. In that gargantuan sample, we would clearly be able to find most, if not all, of the possible charm/bottom states especially the charm strange (or darkly strange) baryons and the exotic bottom states. Not only would such states be observed but most of their branching ratios would be simultaneously measured. We should be able to measure lifetimes as small as 10^{-13} sec. We can observe the spectrum of excited states, along with details of production and decay.

We note in addition that the physics program we envisage for the full detector is by no means restricted to the wealth of data in the S, C, and B systems. The selectivity of our detector will permit us for example to probe deeply into all dissociation phenomena and to study "hard scattering" processes such as jet production. In a real sense, the physics potential of this program is extremely broad.

Requests, Costs, Schedule

The physics program described above requires:

A. Magnets

1. The "Jolly Green Giant" would have to be acquired from BNL and assembled at Fermilab.

2. A small dipole with aperture at least 6 in. square and field integral of at least 500 MeV, required initially for a downstream beam particle spectrometer.

3. Spectrometer magnet M2, aperture 48 x 60 x 72 (hwd) peak field ~ 8 kG.

B. Beam Line

We require a hadron beam capable of deliverying 20 MHz of charged particles, with momentum variable from 200 GeV to full Tevatron energy, with ~ 1% momentum spread. We require a beam diverging from a point source (~ 1 mm diameter) to a diameter of two inches at the detector 200 ft downstream.

C. Beam Time

The multistage program outlined above requires 400 hours of target fragmentation measurements during installation of full spectrometer. 1000 hours of beam with full detector.

D. Costs

Only a modest investment by Fermilab is required. In addition to the beam line and experimental area, we are requesting that Fermilab supply an analyzing magnet and iron for the hadron calorimeter. The cost of the major portions

of the target fragmentation phase is estimated at $400 K. This includes the processor, chambers and Cerenkov counters. (If we run at BNL before coming to Fermilab, this equipment will be tested and operational.)

We estimate the cost of the major additional items as:

Photon/hadron calorimeter:	$400 K
Cerenkov counters C_1, C_2:	150 K
Drift Chambers 7, 8, 9:	200 K
Additional Reconstruction Hardware:	50 K

E. Schedule

We will be ready to take beam as soon as a beam area can be proposed for us (~ early 1984). We would install the pieces of the full detector as they are completed with the full detector assembled by mid-1985.

References

1 J. Aubert et al, Phys. Rev. Lett. 33, 1404 (1974);
J. Augustin et al, Phys. Rev. Lett. 33, 1406 (1974).

2 V.E. Barnes et al, Phys. Rev. Lett. 12, 204 (1964).

3 M.K. Gaillard et al, Rev. Mod. Phys. 47, 277 (1975).

4 G. Goldhaber et al, Phys. Rev. Lett. 37, 255 (1976);
I. Peruzziet al, Phys. Rev. Lett. 37, 569 (1976);
G.J. Feldman et al, Phys. Rev. Lett. 38, 1313 (1977);
G. Goldhaber et al, Phys. Lett. B69, 503 (1977);
G.S. Abrams et al, Phys. Rev. Lett. 44, 10 (1980).

5 S. Wojcicki, Madison Conference (1980).

6 R.E. Ansorge et al, Nucl. Phys. B103, 509 (1976).

7 K. Berkelman, Madison Conference (1980);
D. Andrews, Phys. Rev. Lett. 44, 1108 (1980);
T. Bohringer, Phys. Rev. Lett. 44, 1111 (1980).

8 H. Fritzch, K. Streng, Phys. Lett. 78B, 447 (1978).

9 W. Lockman et al, XVIII Int. Conf. on High Energy Physics, Tbilisi (1976).

10 J. Whitmore, Phys. Reports 10C, 300 (1974).

11 J.W. Chapman et al, Phys. Rev. Lett. 32, 257 (1974).

12 Y. Akimov et al, Phys. Rev. Lett. 35, 763 (1975).

13 M.G. Albrow et al, Nucl. Phys. B108, 1 (1976).

14 S. Childress et al, Phys. Lett. 65B, 177 (1976).

15 D.S. Ayres et al, Phys. Rev. Lett. 37, 1724 (1976).

16 R. Webb et al, Phys. Lett. 55B, 331 (1975).
V. Blobel et al, Nucl. Phys. B92, 221 (1975).

[17] L. Baksay et al, Phys. Lett. 61B, 405 (1976).
B. Lockman et al, Particles and Fields, p. 213, (1975), U. of Washington, Seattle.

[18] J. Hofmann et al, Nucl. Phys. B125, 404 (1977).

[19] Illinois-Fermilab-Harvard-Oxford-Tufts Collaboration, paper submitted to Madison Conference (1980).

[20] K.L. Giboni et al, Phys. Lett. B85, 437 (1979).
W. Lockman et al, Phys. Lett. B85, 443 (1979).
D. Dryard et al, Phys. Lett. B85, 452 (1979).

[21] R.L. Anderson, IEEE NS-25, 340 (1978).

Table 1: Magnetic Spectrometer

Magnet	Aperture (hwd)	Field Integral
M1	48 in. x 96 in. x 90 in.	400 MeV
M2	48 in. x 60 in. x 72 in.	600 MeV

Chamber	Distance From Target (in.)	Dimension H x W (in.)	Wire Spacing (mm)	# of Wires
1	6	24 x 36	2	3 x 450
2	12	24 x 36	2	3 x 450
3	24	40 x 60	3	3 x 480
4	36	40 x 60	3	3 x 480
5	60	40 x 60	3	3 x 480
6	84	48 x 72	4	3 x 450
7	120	72 x 80	4	3 x 500
8	252	48 x 66	4	3 x 410
9	474	96 x 96	6	3 x 384
				12,252

Table 2

Cerenkov Counter	C_0	C_1	C_2
Radiator	C_4H_{10}	N_2	N_2/H_c
$(n-1)\times10^6$	1200	300	75
Pion Threshold	3	6	12
Length of Radiator	24 in.	100 in.	180 in.
Downstream Size (in.)	6 x 80	48 x 60	96 x 96
Number of Phototubes	116	116	105
θ_c	50 mr	25 mr	12 mr
# of Photoelectrons	8	8	8

Segmentation

C_0, C_1

4	4	4	4	4
4	9	12	9	4
4	9	12	9	4
4	4	4	4	4

4 =

9 =

12 =

C_2

4	4	4	4	4
4	4	4	4	4
4	4	9	4	4
4	4	4	4	4
4	4	4	4	4

Table 3:

Photon Calorimeter

3 modules, each 8 radiation lengths, 16 samples transverse segmentation:

1) 4 ft x 4 ft quadrants

2) 1 cm strips alternately horizontal and vertical

Total segmentation 500 strips per view, each module or 3,000 analog measurements.

Hadron Calorimeter

2 modules, identical to photon calorimeter, except for 6 mm Fe replacing 3 mm Pb.

Followed by 48 in. of iron (9 ft square cross section)

24 samples: cathode readout MWPC in 32 x 32 rectangular grid

Total segmentation 3,000 analog measurements.

Table 4: Detection Efficiency

(X-Production Given by $\frac{d\sigma}{dP_t^2} = e^{-7P_t^2}$)

$pp \to pX$ $X \to$	Mass Thres-hold	M_X 2.0	2.5	3.0	3.5	4.0	4.5	5.0	6.0
$p\pi^+\pi^-\pi^+\pi^-$	1.50	.01	.01	.03	.05	.09	.13	.19	.30
$\Lambda^o K^+$ $\hookrightarrow p\pi^-$	1.61	.04	.05	.09	.13	.18	.22	.25	.29
$\Lambda^o K^o \pi^+$ $\hookrightarrow \pi^+\pi^-$ $\hookrightarrow p\pi^-$	1.76	.01	.02	.03	.06	.09	.13	.17	.20
$p\pi^+\pi^-\pi^+\pi^-\pi^+\pi^-$	1.78	.00	.01	.02	.03	.05	.09	.15	.23
$\Lambda^o K^+\pi^+\pi^-$ $\hookrightarrow p\pi^-$	1.89	.07	.05	.07	.09	.13	.17	.22	.29
pK^+K^-	1.93	.80	.18	.17	.21	.27	.34	.41	.53
$pK^o\bar{K}^o$ $\hookrightarrow \pi^+\pi^-$ $\hookrightarrow \pi^+\pi^-$	1.93	.01	.02	.03	.05	.09	.13	.17	.24
$\Lambda^o K^o \pi^+\pi^-\pi^+$ $\hookrightarrow \pi^+\pi^-$ $\hookrightarrow p\pi^-$	2.04	-	.01	.02	.03	.05	.09	.13	.21
$p\bar{K}^o K^+\pi^-$ $\hookrightarrow \pi^+\pi^-$	2.07	-	.06	.07	.09	.13	.19	.23	.32
$\Lambda^o K^+\pi^+\pi^-\pi^+\pi^-$ $\hookrightarrow p\pi^-$	2.17	-	.07	.05	.06	.08	.11	.15	.24
$\Lambda^{o*}(1690)K^+$ $\hookrightarrow \Lambda^o\pi^+\pi^-$ $\hookrightarrow p\pi^-$	2.19	-	.04	.06	.10	.14	.20	.26	.33
$pK^+K^-\pi^+\pi^-$	2.21	-	.26	.17	.18	.20	.25	.30	.42

$pp \to px$ $X \to$	Mass Threshold	M_X 2.5	3.0	3.5	4.0	4.5	5.0	6.0
$\Xi^- K^+ K^+$ $\hookrightarrow \Lambda^o \pi^-$ $\hookrightarrow p\pi^-$	2.31	.27	.15	.14	.17	.21	.22	.24
$p\bar{K}^o K^+ \pi^+ \pi^- \pi^-$ $\hookrightarrow \pi^+ \pi^-$	2.35	.05	.06	.07	.09	.13	.19	.28
$\Xi^- K^o K^+ \pi^+$ $\hookrightarrow \pi^+ \pi^-$ $\hookrightarrow \Lambda^o \pi^-$ $\hookrightarrow p\pi^-$	2.46	-	.04	.07	.09	.12	.15	.19
$\Lambda^{o*}(1690) K^+ \pi^+ \pi^-$ $\hookrightarrow pK^-$	2.47	-	.16	.17	.21	.26	.32	.43
$pK^+ K^- \pi^+ \pi^- \pi^+ \pi^-$	2.49	-	.19	.15	.16	.20	.25	.33
$\Lambda^{o*}(1690) K^+ \pi^+ \pi^+ \pi^- \pi^-$ $\hookrightarrow pK^-$	2.75	-	.03	.04	.06	.09	.13	.21
$pp\bar{p}$	2.82	-	.99	.81	.68	.65	.64	.69
$pp\bar{p}\pi^+ \pi^-$	3.10	-	-	.57	.51	.50	.53	.58
$\Omega^- K^o K^+ K^+$ $\hookrightarrow \pi^+ \pi^-$ $\hookrightarrow \Lambda^o K^-$ $\hookrightarrow p\pi^-$	3.16	-	-	.35	.30	.29	.31	.33
$p\Lambda^o \bar{\Lambda}^o$ $\hookrightarrow p\pi^-$ $\hookrightarrow p\pi^-$	3.17	-	-	.64	.53	.45	.39	.32
$p\Xi^- \bar{\Xi}^-$ $\hookrightarrow \bar{\Lambda}^o \pi^+$ $\hookrightarrow \Lambda^o \pi^-$ $\hookrightarrow \bar{p}\pi^+$ $\hookrightarrow p\pi^-$	3.58	-	-	-	.43	.34	.27	.18

$pp \to px$ $X \to$	Mass Threshold	M_X 4.5	5.0	6.0
$\Lambda_c^+ \bar{D}^o$ $\hookrightarrow K^+\pi^-$ $\hookrightarrow pK^-\pi^+$	4.14	.25	.30	.43
$\Lambda_c^+ \bar{D}^o$ $\hookrightarrow K^+\pi^-$ $\hookrightarrow \Lambda^o\pi^+\pi^-\pi^+$ $\hookrightarrow p\pi^-$	4.14	.12	.16	.26
$\Lambda_c^+ D^-\pi^+$ $\hookrightarrow K^+\pi^-\pi^-$ $\hookrightarrow pK^-\pi^+$	4.29	.19	.22	.32
$p\Omega^- \bar{\Omega}^=$ $\hookrightarrow \bar{\Lambda}^o K^+$ $\hookrightarrow \Lambda^o K^- \to \bar{p}\pi^+$ $\hookrightarrow p\pi^-$	4.29	.75	.66	.49
$\Sigma_c^{++} D^-$ $\hookrightarrow K^+\pi^-\pi^-$ $\hookrightarrow pK^-\pi^+\pi^+$	4.30	.19	.23	.35
$\Sigma_c^{++} D^-$ $\hookrightarrow k^o\pi^-$ $\hookrightarrow \pi^+\pi^-$ $\hookrightarrow p\bar{K}^o\pi^+$ $\hookrightarrow \pi^+\pi^-$	4.30	.08	.13	.21
$\Sigma_c^{++} D^-$ $\hookrightarrow K^+\pi^-\pi^-$ $\hookrightarrow p\bar{K}^o\pi^+$ $\hookrightarrow \pi^+\pi^-$	4.30	.12	.16	.28
$\Lambda_c^+ \bar{D}^o \pi^+\pi^-$ $\hookrightarrow K^+\pi^-$ $\hookrightarrow pK^-\pi^+$	4.42	.27	.24	.33

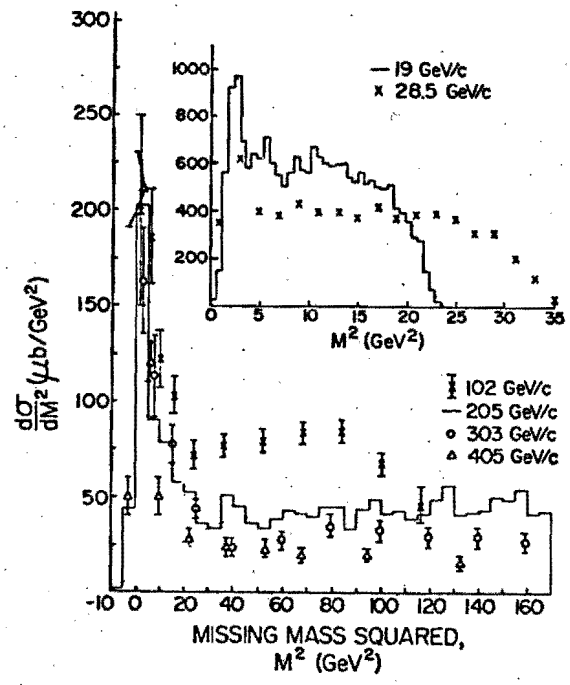

Fig. 29. Missing mass squared distributions for inelastic events from the reaction pp → slow p + anything. The dashed curves represent hand drawn backgrounds used to estimate diffractive cross sections at 102 and 205 GeV/c.

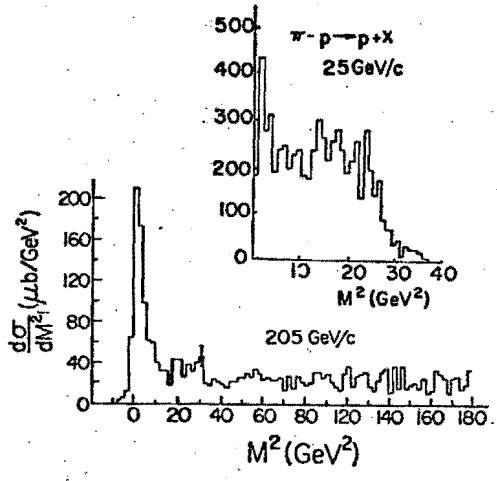

Fig. 30. Missing mass squared distributions for inelastic events from the reaction $\pi^-p \rightarrow$ slow p + anything.

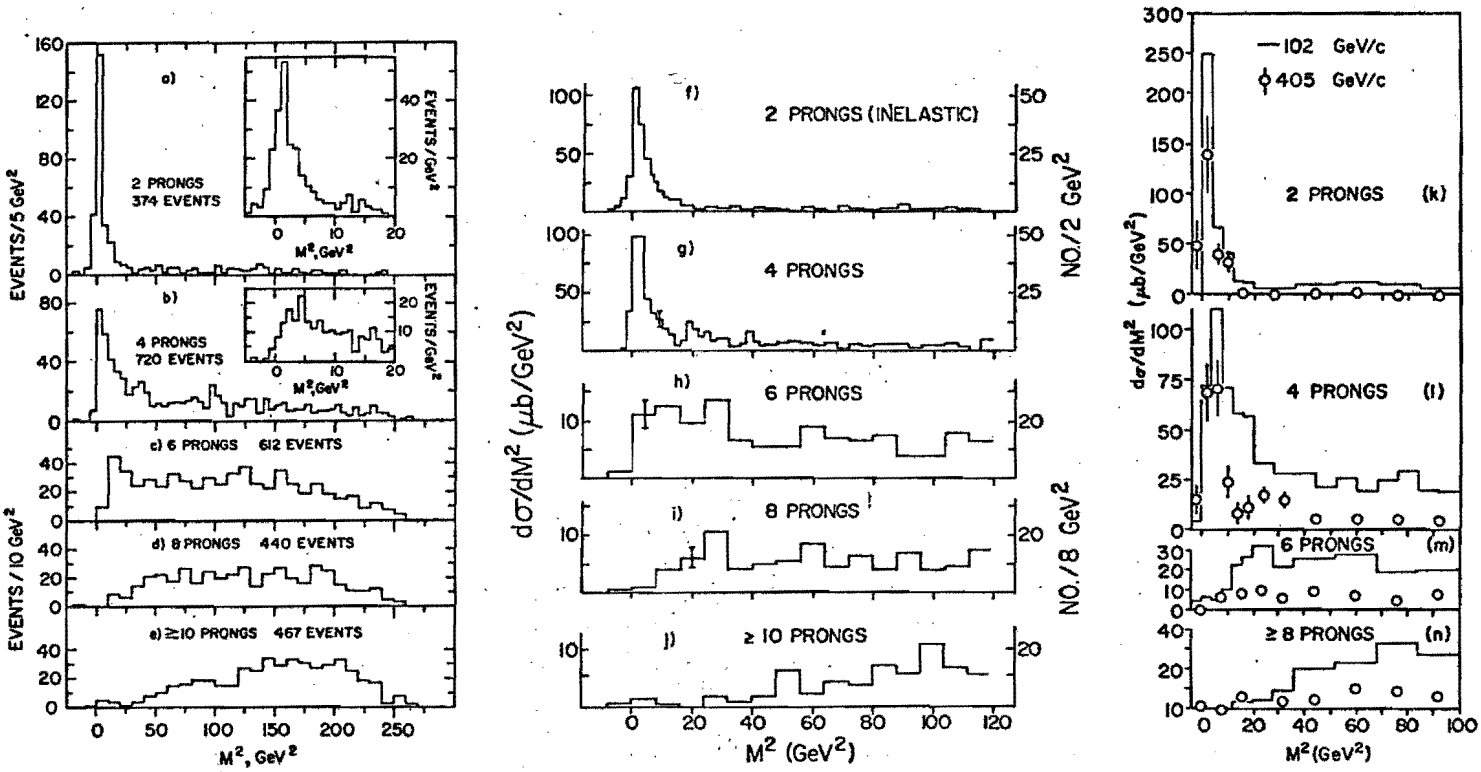

Fig. 31. Missing mass squared distributions for various topologies. (a) to (e) for the reaction pp → slow p + anything at 205 GeV/c. (f) to (j) for the reaction $\pi^-p \rightarrow$ slow p + anything at 205 GeV/c. (k) to (n) for the reaction pp → slow p + anything at 102 and 405 GeV/c.

Fig. 1

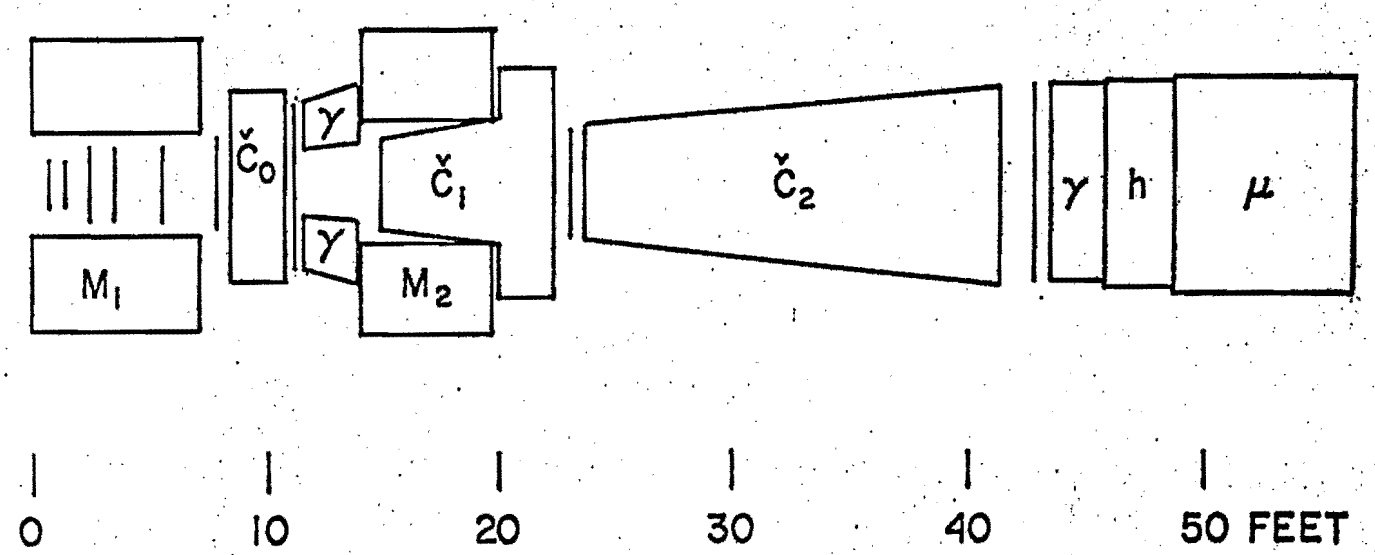
M_1
$\check{C}_0$
γ
γ
$\check{C}_1$
M_2
$\check{C}_2$
γ
h
μ
0
10
20
30
40
50 FEET

FIG. 2

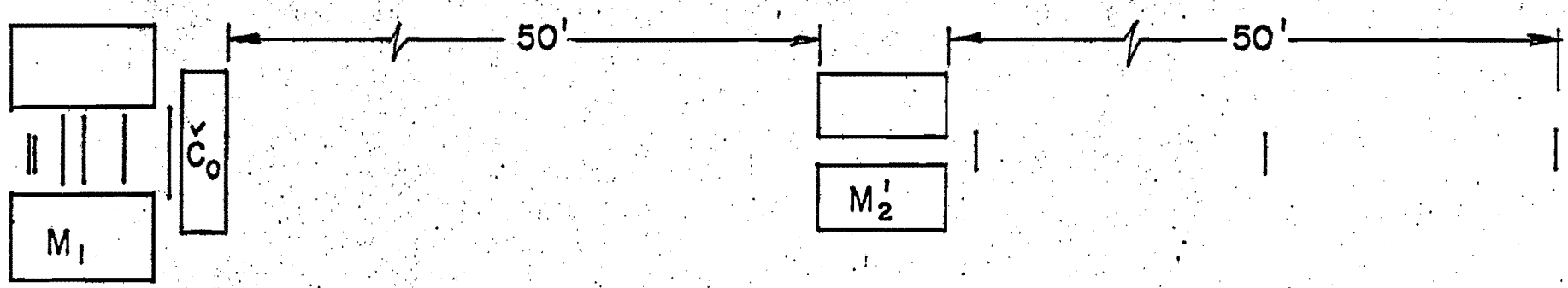

FIG. 3